

EXPERIMENTAL RESEARCH OF PARTIAL REGULAR MICRORELIEFS FORMED ON ROTARY BODY FACE SURFACES

Volodymyr DZYURA¹, Pavlo MARUSCHAK^{1*}, Stoyan SLAVOV²,
Diyan DIMITROV³, Dimka VASILEVA²

¹*Department of Industrial Automation, Ternopil Ivan Puluji National Technical University, 46001 Ternopil, Ukraine*

²*Department of Manufacturing Technologies and Machine Tools, Technical University of Varna,
9010 Varna, Bulgaria*

³*Department of Mechanics and Machine Elements, Technical University of Varna, 9010 Varna, Bulgaria*

Received 4 June 2021; accepted 27 July 2021

Abstract. The basic regularities in the influence of processing parameters on the geometrical characteristics of the partially regular microreliefs, formed on the rotary body face surface, are established. Combinations of partially regular microreliefs are formed by using a contemporary CNC milling machine, and an advanced programming method, based on previously developed mathematical models. Full factorial experimental design is carried out, which consist of three factors, varied on three levels. Regression stochastic models in coded and natural form, which give the relations between the width of the grooves and the deforming force, feed rate and the pitch of the axial grooves, are derived as a result. Response surfaces and contour plots are built in order to facilitate the results analysis. Based on the dependencies of the derived regression stochastic models, it is found that the greatest impact on the width of the grooves has the magnitude of the deforming force, followed by the feed rate. Also, it is found that the axial pitch between adjacent toolpaths has the least impact on the width of the grooves. As a result of the full-factorial experiment, the average geometric parameters of the microrelief grooves were obtained on their basis. When used, these values will provide for the required value of the relative burnishing area of the surface with regular microreliefs, and, accordingly, the specified operational properties.

Keywords: aircraft hydraulic systems, ball burnishing, technological parameters, regular microreliefs.

Introduction

Many vehicles and machines used in different industries and for various functional purposes employ a number of parts that work by using their face surface. Such parts include conical disks of variators, embedded in the automatic transmissions of cars and harvester combines, parts of tapered and axial bearings, aircraft turbocharger flanges, valves of gas-distributing mechanisms in internal combustion engines, sleeves and rods of hydraulic systems, etc. (Wang et al., 2016; Ouyang et al., 2011; Diltemiz et al., 2009; Pogodayev, 2004).

Hydraulic cylinders are traditionally used in aviation:

1) to create significant mechanical effort during bench tests of aircraft. They are widely used for testing aircraft when it is necessary to reproduce flight alternating loads. Hydraulic cylinders mounted on the stand pull and push the wing of the aircraft up and

down, simulating the load during the flight (Vorontkov, 2019);

2) in chassis designs for aircraft of different types: transport aircraft (Tu-204SM), helicopters: Ka-25, Ka-27, Ka-62, civil aviation aircraft: An-148, IL-86, IL-96, An-24, Tu-134, Tu-204, Tu-214 (Korneev, 2009);

3) in designs of ground towing devices of aircraft (Lazarev et al., 2008).

Stringent requirements are placed on the wear resistance of the contact surfaces of such parts, which in the long run provide for their service lifetime and efficiency.

Surfaces with regular microreliefs (RMR) could be used as an element for the contact surfaces of such parts, subjected to stringent requirements in terms of assuring the needed accuracy between the conjugate surfaces. Such workpieces are also used in mechanisms like spool valves for oil and hydraulic systems in the aircraft, like

*Corresponding author. E-mail: maruschak.tu.edu@gmail.com

aileron control system, chassis release, and other systems. The plastic deformation of the surface layer in order to strengthen it, combined with the formation of certain RMR onto it, appears to be a prospective method for improving the physical and mechanical properties of its contact surfaces (Dzyura et al., 2017). The contemporary metal cutting machines controlled by a computer numerical control (CNC) system make it possible to significantly expand the scope of application of such methods. For example, CNC milling (or lathe) machines are capable to form RMR of different types onto surfaces with different shape and size, without the need of a forced additional vibration (Slavov et al., 2021). This allows the ball burnishing operation to be applied as a finishing processing of the contact surface of the part, within the typical operation sequence, using much simpler deforming tools, in comparison with the classical approaches for RMR formation.

One of the important RMR parameters is its relative area, i.e., the ratio of the area occupied by microrelief grooves and the total surface area, on which it is formed. This parameter mainly determines the performance properties of the surface with a partially regular microrelief. As shown by previous studies (Leshkenova, 2002), the width of the microrelief groove has the greatest influence on the relative area variation. Mathematical models of RMR are first defined by (Schneider, 1984), where the conditions for obtaining partially RMR of types I-III are derived. These studies have become the basis for developing GOST 24773-81 standard, which specifies the RMR parameters formed on flat and cylindrical surfaces. The positive effect of RMR on the operational properties of the surface is confirmed by many researchers from various fields of science.

In particular, the RMR applied to the inner cylindrical surface of the rod pump plunger pair is found to significantly enhance the tightness of the movable joint and, consequently, its service life, as shown in Bakhtizin et al. (2017).

This is confirmed by research findings presented in Radionenko et al. (2018), Kindrachuk et al. (2014). The authors have found that the use of RMR with different geometric parameters can influence the friction and lubrication conditions of the conjugate friction surfaces, thus preventing unacceptable conditions, in which the contact surface will be damaged. The ability to adjust the friction conditions of the workpiece surfaces is also an important prerequisite to achieve high reliability, long service life, and work efficiency of major aircraft equipment used. RMR can be applied onto surfaces of high-precision components and units with conjugated relatively moving parts, such as, for instance, valves of oil and hydraulic systems, pump gear ends shielded by the elements of internal combustion engines, and other equipment.

Research findings with regard to various-shape RMR grooves formed on the specimen surface, which affect the friction coefficient, the temperature in the friction zone and the surface ability to retain lubricants and wear prod-

ucts, are presented in Wu et al. (2016). The reduction of the friction coefficient leads to a reduced consumption of energy for driving the mechanisms, which can be very relevant in the aviation industry, as well as in any other vehicle industry.

In Zhang et al. (2019), research findings are presented, which indicate that a microrelief microstructure formed on the inner cylindrical surface of the cylinder liner, contributes to the ability of this surface to retain the oil film. This property of the working surface of the cylinder liner improves the operational properties of the surface and extends the cylinder life, as a whole.

The results of the theoretical and experimental studies summarized in Stadnychenko and Varvarov (2019) are related to the tribosystems' transition from normal to "abnormally low" friction, considering the thermodynamics. The reason for this transition is that the microrelief is characterized by certain parameters, which are formed on the contact surface. This type of microrelief creates conditions for micro-contact quasi-elastic interaction.

Improving the anticorrosive properties of the surface of magnesium alloy (Mg Alloy AZ31) after surface treatment by plastic deformation in a manner close to the ball burnishing method is described in Cao et al. (2020), where the authors have conducted experimental studies using the Taguchi approach.

To determine experimentally the influence of a group of different factors on one or more dependent parameters, it is advisable to conduct a full-factorial experiment. For contemporary mechanical engineering, conducting experimental research in order to study the influence of individual factors can be quite expensive. Therefore, a full-factorial experiment that involves simultaneous changes of all studied factors is the most efficient solution. Designing and conducting a full-factorial experiment is described in detail in Krishnaiah and Shahabudeen (2012), Dyshunskyi (1998).

The practical use of the full-factorial experiment approach applied in the experimental investigation into the effect of the machining regime parameters on the quality parameters in blade machining is described in Hamdi et al. (2020), Nalbant et al. (2007), Zerti et al. (2017).

Similar experimental investigation is described in detail in Slavov and Dimitrov (2018), Slavov et al. (2020), where the results of a full-factorial experiment with four factors (i.e. the feed rate, the deforming force, the amplitude of the deforming element and the number of oscillations) are presented. According to the research findings, Pareto histograms are constructed, which show that the number of oscillations and the amplitude of the deforming element have a significant effect on the shape variation of the RMR cells.

An experimental investigation into the effect of ball vibroburnishing conditions on the main dimensional characteristics of the RMR grooves is conducted (Nagit et al., 2020). The input factors of the process are the ball diameter, the force and speed of the workpiece rotation.

The depth and width of the grooves formed by the balls onto the surface layer of the workpiece are measured, and empirical mathematical dependences are derived by mathematical processing of the experimental results. These dependences indicate the impact of the input factors of the vibration processes on the geometric parameters of the groove. However, in this study, the influence of the feed rate as a processing parameter on the geometric parameters of the groove is not defined.

The results of the experimental investigation into the RMR formation, followed by chromium plating of a flat surface, are presented in Kyrychok and Lototska (2011). The authors have developed an algorithm for controlling the technological process of RMR formation by plastic deformation of flat surfaces of printing equipment parts. The algorithm takes into account a set of indicators related to the material, geometrical and physical-mechanical parameters, and the conditions of plastic deformation of the surface. Depending on the material hardness and the RMR's geometry, the algorithm selects the geometry and the parameters of the deforming tool. The material hardness is used to calculate the pressing force of the tool. The authors choose such parameters as the indentation force of the deforming element, its radius and the thickness of the chromium layer deposited on the surface. These studies are interesting because they aim at developing the processing technology for RMR formation and provide the improved performance of the working surfaces of cylindrical parts.

In the contemporary machine-building production, CNC milling machines are increasingly used to form RMR. In (Kuzmin et al., 2015), the authors suggest the technology of applying RMR on a flat surface, using a CNC milling machine. The equation of the tool center movement versus the input parameters is presented. The technique of creating a numerical control (NC) code for Siemens and Fanuc CNC systems for RMR formation by plastic deformation on flat surfaces is described. To visualize the obtained microrelief, a WinNC simulator developed by EMCO (Austria) is used.

It is noteworthy that the deformation rate has a significant impact on the surface layer quality in a fairly wide range (Schneider, 1984). As the deformation rate increases, the amount of plastic deformation increases too, and the roughness of the treated surface decreases. However, this dependence has an optimum character. Finding the optimal value of the deformation rate, in which the roughness still has minimal height, is considered an important research problem in this field. This could be an opportunity to increase the ball burnishing operation productivity. Determining the functional relationship between the deforming force applied to the tool and the quality parameters of a workpiece is one of the main research objectives in the field of surface layer plastic deformation (i.e. ball burnishing operation).

The main objective of the current research is to obtain a regression stochastic model between the main parameters of the ball-burnishing operation: deforming force,

feed rate, the axial step between adjacent RMR grooves, and the width of RMR grooves, that will provide the required relative area of the surface vibration with regular microreliefs, and, accordingly, the specified operational properties.

1. Description of the experimental setup for partially regular relief formation

Experimental study is conducted in order to test two theoretical hypotheses, in particular:

- 1) to confirm the correctness of the derived mathematical models that describe partial RMRs formed on the faces of the rotary body and given in Dzyura (2020);
- 2) to determine the influence of the regime parameters which characterize the partial RRM formation process, such as deforming force magnitude, feed rate of the deforming tool movement, and partial RMR geometrical parameter (i.e. the axial pitch between the microrelief grooves), on the width of plastically deformed grooves obtained after applying the ball burnishing operations.

The experimental studies are performed using a test specimen made of steel C45 (EN 10083-2), which is shown in Figure 1. To obtain the coordinates required for constructing the V-shaped cyclogramic toolpaths of the ball tool, a derived mathematical model is used (Dzyura, 2020).

$$\begin{cases} x_{in} = r_n \cdot \cos(\varphi_i); \\ y_{in} = r_n \cdot \sin(\varphi_i); \\ x_k = 0,2 \cdot \pi \cdot A_k \cdot \arcsin[\sin((\varphi_i + \gamma_d) \cdot n_{el})] \cdot \cos(\varphi_i) + x_{in}; \\ y_k = 0,2 \cdot \pi \cdot A_k \cdot \arcsin[\sin((\varphi_i + \gamma_d) \cdot n_{el})] \cdot \sin(\varphi_i) + y_{in}, \end{cases} \quad (1)$$

where $r_n = r_{n-1} + S_0$; $\gamma_d = 0$.

A_k – amplitude of microrelief grooves, mm; r_n – radius of axial lines of continuous regular microroughnesses, mm; x_{in} , y_{in} – coordinates of axial lines of continuous regular microroughnesses, mm; φ_i – instantaneous value of the angle when determining the coordinates of the axial lines of continuous regular micro-irregularities, deg; γ_d – the displacement angle of the axial lines of symmetry of the grooves, which have different radii of the axial lines of continuous regular micro-irregularities, deg; r_{el} – the number of groove elements placed on the circle radius r_n .

In order to form partial RMRs on the test specimen faces, which have specific characteristics, the points from the toolpaths shown in the Figure 2 are calculated by using this mathematical model.

The shape and dimensions of the test specimen (see Figure 1) are designed to provide large enough surface segments for all experimental toolpaths (see Figure 2) and in accordance with the technical specification of the production equipment used. Both specimen faces are previously machined by finishing turning before they are subjected to ball burnishing processing. As can be seen from Figure 2, one of the face surfaces is split into four

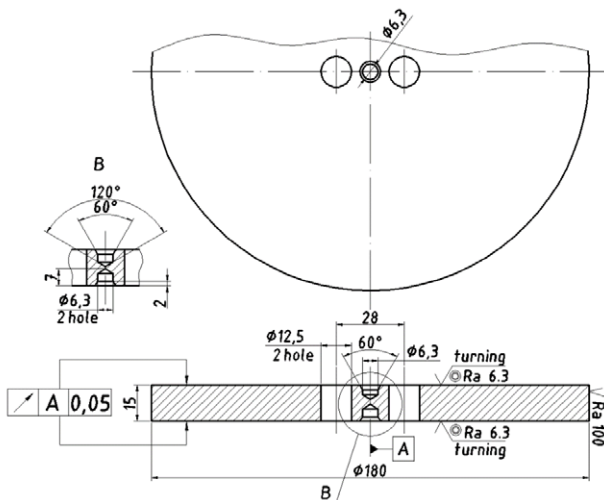


Figure 1. Test specimen shape and dimensions

sections (Figure 2, a) and c) and another one is split into five sections (Figure 2, b) and d)). In this way, the specimen provides enough useful surface area for conducting a full-factorial experimental design with three factors. All nine sections provide the needed 27 areas with partial RMR formed under all combinations of the ball burnishing factor's levels according to the chosen experimental design (see Table 1). All toolpath coordinates are calculated by using an algorithm written in MathCAD based on mathematical models described in (Dzyura, 2020).

The machine tool equipment of the Department of Manufacturing Technologies and Machine Tools of the Technical University of Varna (Bulgaria) is used for conducting the physical experimental research. In particular, all ball burnishing operations are carried out on the HAAS TM-1 milling machine with CNC. A specially designed tool for ball burnishing adapted to work along with CNC equipment is used to form the partially regular microrelief (see Figure 3).

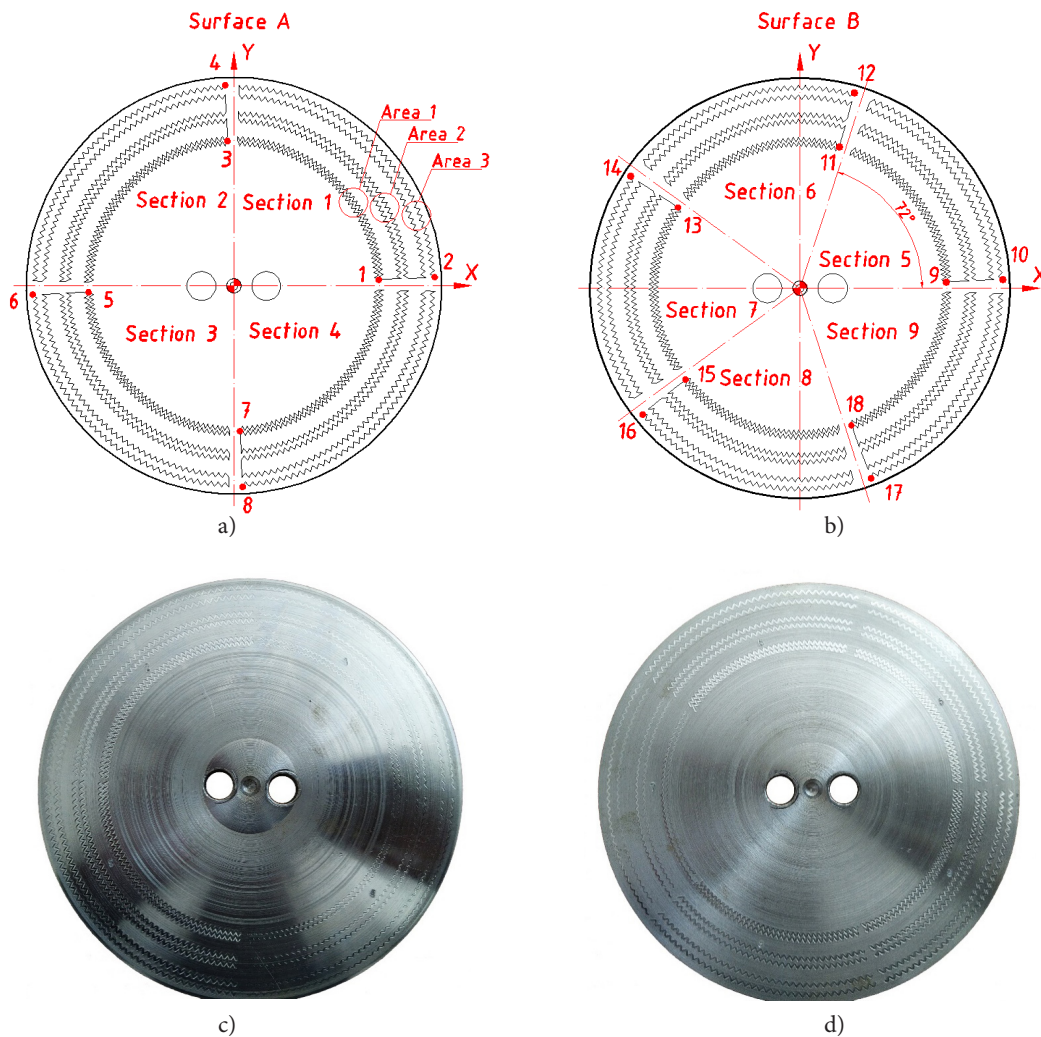


Figure 2. Test specimen with marked points of the toolpath and sections: 1–2,...17–18 – the beginning and end points of the toolpath trajectory during the partial RMR formation; a), c) surface A of the test specimen; b), d) surface B of the test specimen

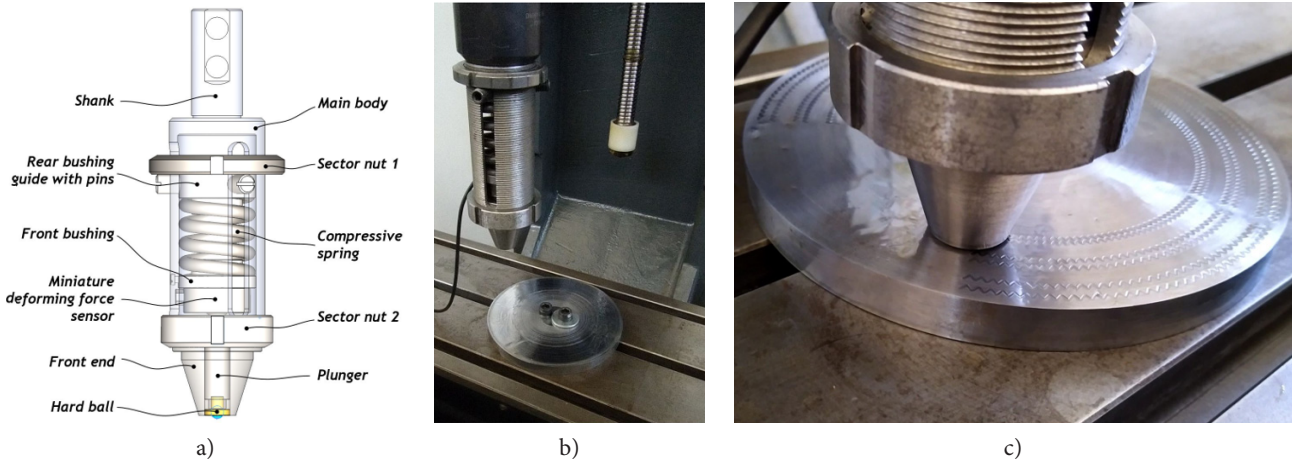


Figure 3. Obtaining regular reliefs by ball burnishing (Slavov & Iliev, 2016): a) construction of the burnishing tool for forming RMRs; b) experimental setup for obtaining regular reliefs by ball burnishing; c) partially regular reliefs formed on flat surface of the test specimen by using the burnishing tool

The deforming tool used in the current experimental investigation is capable of providing a deforming force of up to 3200 N and can be adjusted precisely by changing the compression of the spring and by using the integrated miniature force sensor for its measurement (see Figure 3, a). The measured deforming force can be recorded in real time on the (external) computer for further analysis. The ball diameter is 6 mm for all ball burnishing operations conducted in the experimental research. Ball parameters are stipulated by GOST 3722-2014. The balls are heat treated, and their hardness is from 82.3 to 84.5 HRA.

Deforming force magnitudes, tool feed rates and axial pitches of the grooves are chosen as variables. It is expected that these factors will have a significant effect on the width variability of the formed groove and, accordingly, the area of partially regular microrelief formed on the flat faces. In addition, these parameters are interdependent and can be easily amended during the ball burnishing operations. According to the recommendations given in Schneider (1984); Nalbant et al. (2007), the deforming force ranges from 200 N to 600 N in order to achieve the deformation rates needed.

The effect of the axial step S_o on the groove width b_k (see Figure 5, d) is only possible when its value is small enough, and the grooves are placed close enough to each other. Therefore, the axial step is in the range between 2 and 4 mm with a pitch of 1 mm. The geometrical parameters of the partial RMR grooves are the same for all areas and sections of the specimen: amplitude – $A_k = 1$ mm; number of elements in the interval $0...2\pi$: $n_{el} = 180$ pcs.; displacement coefficient – $\gamma_d = 0$; the shape of the partial RMR grooves is triangular. The toolpaths during the ball burnishing operations are shown schematically in Figure 4.

As follows from the analysis of the previous research findings (Schneider, 1984; Kyrychok & Lototska, 2011), the groove formation process, which is the subject of the

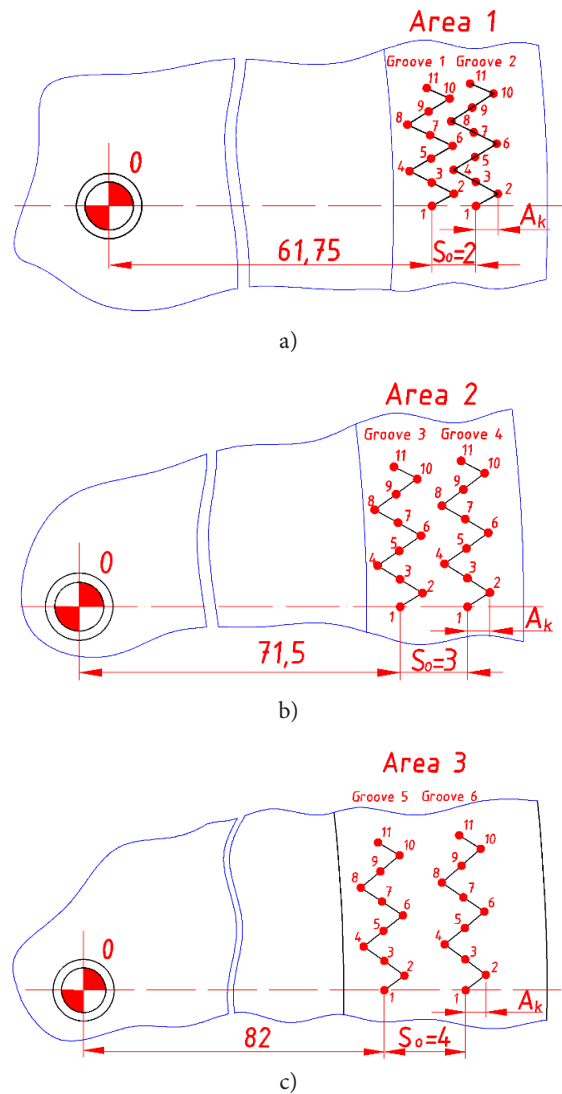


Figure 4. Toolpaths defined by the coordinate points in the ball burnishing operations: a) in zone 1 at $S_o = 2$ mm; b) in zone 2 at $S_o = 3$ mm; c) in zone 3 at $S_o = 4$ mm

current study, cannot be described by a linear model. This is because the response surface is dominated by regression equations that characterize the interaction effects and quadratic forms. To describe this relationship, it is necessary to use second-order regression equations, in which each variable must vary at least at three levels. Generally, the second-order regression equation for three factors can be written as follows (Nalbant et al., 2007):

$$b_k = b_0 + b_1x_1 + b_2x_2 + b_3x_3 + b_{12}x_1 \cdot x_2 + b_{13}x_1x_3 + b_{23}x_2x_3 + b_{11}x_1^2 + b_{22}x_2^2 + b_{33}x_3^2, \quad (2)$$

where: b_k is the sample estimation of the function studied (i.e. the width of the partial RMR groove formed on the rotary body faces in the present research);

$b_0, b_1, b_2, b_3, b_{12}, b_{13}, b_{23}, b_{11}, b_{22}, b_{33}$ are the sample coefficients of the regression equation (or the so called “regressors”);

x_1, x_2, x_3 are the independent variables, which in this case correspond to the main regime parameters of the ball bur-

nishing operation: axial step between grooves S_o , deforming force F_d and feed rate f_i .

Onto each of the above described nine sections, corresponding partially regular microrelief with characteristics shown in Table 1 was applied by ball burnishing using the deforming tool shown in Figure 3.

The value of parameter b_k is obtained by measurement using digital images with high resolution (Figure 5) for each of the 27 zones (areas) of the test specimen. A Digi Micro Lab 5.0+ digital microscope is used for that purpose.

Table 1. Values of variable parameters for the experimental research conducted

Experiment number	Section	Area	Axial step of grooves, $S_{o,p}$ mm	Deforming force, $F_{d,p}$ N	Feed rate, $f_{in,p}$ mm/min
1	1	1	2	200	500
2		2	3	200	500
3		3	4	200	500
4	2	1	2	400	500
5		2	3	400	500
6		3	4	400	500
7	3	1	2	600	500
8		2	3	600	500
9		3	4	600	500
10	4	1	2	200	1000
11		2	3	200	1000
12		3	4	200	1000
13	5	1	2	400	1000
14		2	3	400	1000
15		3	4	400	1000
16	6	1	2	600	1000
17		2	3	600	1000
18		3	4	600	1000
19	7	1	2	200	1500
20		2	3	200	1500
21		3	4	200	1500
22	8	1	2	400	1500
23		2	3	400	1500
24		3	4	400	1500
25	9	1	2	600	1500
26		2	3	600	1500
27		3	4	600	1500

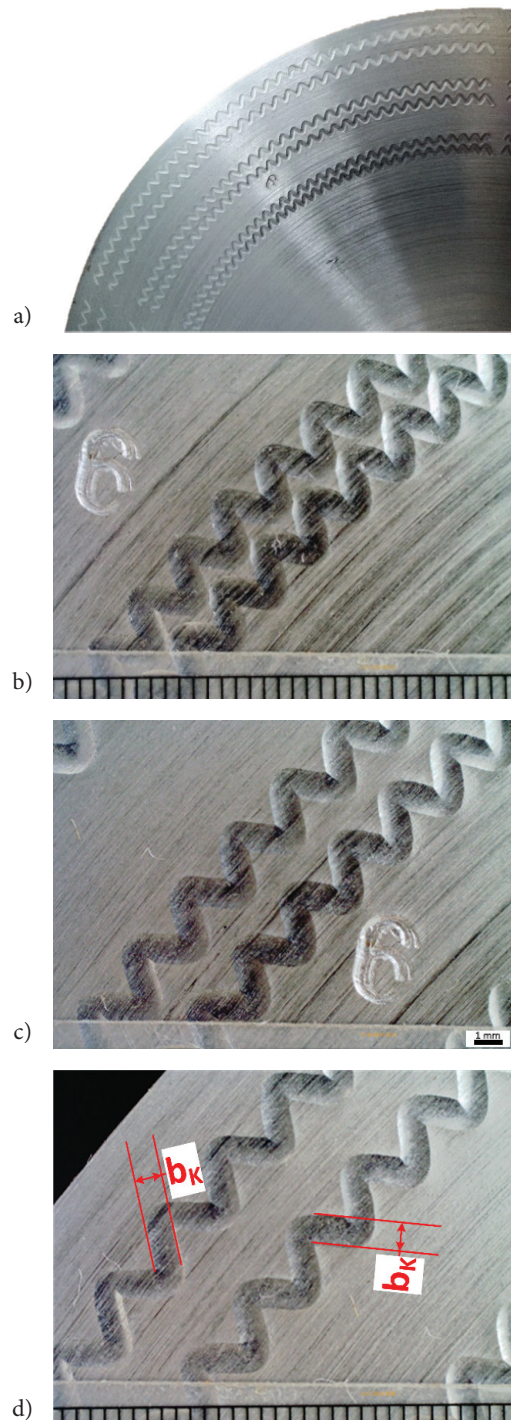


Figure 5. Partially RMR formed on rotary body face surface with a different axial pitch: a) general view of Section 9; b) at $S_o = 2$ mm; c) at $S_o = 3$ mm; d) at $S_o = 4$ mm

Using Portable Capture Pro software, the actual dimensions of the groove widths $b_{k,i,j}$ are measured. Before measuring the partial RMR parameters of the cells, every image captured is calibrated using the etalon calibration ruler in accordance with the manufacturer's calibration methodology.

2. Results from the experimental research

The analyzed dependences of the groove width on the axial distance, the deforming force and the feed rate show that the higher impact parameter is the deforming force. The increase over the entire range of the experimental studies leads to a monotonic nonlinear increase in the width of the groove formed.

To obtain reliable research results, statistical samples from ten measurement of the studied parameter are formed – the groove width $b_{k,i,j}$ – where i is the ordinal number of the experiment ($I = 1..27$), j is the ordinal number

of the groove width measurement ($j = 1..10$). Thus, 270 values of parameter $b_{k,i,j}$ are obtained. The statistical series formed are checked for outliers according to Grubbs' test (Kolker, 1976). If the statistical series prove to be inhomogeneous, the outlier is removed, and an additional measurement of parameter $b_{k,i,j}$ is made. Then, using the small sample theory (Kryvyi et al., 2014), which is used for statistical samples with a small number of values, the mathematical expectation of the parameter $b_{k,i}$ for each experiment, which is approximately equal to the average value, is determined. The results are summarized in Table 2.

After obtaining parameter b_k for each of the experiments, the regression coefficients are derived, and a stochastic mathematical model is built, which describe the influence of axial step of grooves, deforming force and feed rate on that parameter.

Below is the groove width regression equation with coded coefficients depending on the variation of the axial

Table 2. The results of experimental studies of parameter b_k

Meas. number Exp. number	Groove width, $b_{k,i,j}$ mm										Sampling characteristics $b_{k,i,j}$ mm	
	1	2	3	4	5	6	7	8	9	10	Mean (b_k)	Dispersion (b_k)
1	0.57	0.56	0.54	0.56	0.54	0.53	0.56	0.56	0.54	0.53	0.544	1.214×10^{-4}
2	0.57	0.59	0.57	0.55	0.58	0.57	0.54	0.59	0.55	0.56	0.567	1.470×10^{-4}
3	0.59	0.58	0.55	0.61	0.58	0.56	0.58	0.61	0.53	0.62	0.584	8.301×10^{-4}
4	0.85	0.82	0.82	0.84	0.83	0.84	0.85	0.87	0.84	0.86	0.846	1.403×10^{-4}
5	0.85	0.86	0.86	0.88	0.87	0.85	0.84	0.87	0.86	0.84	0.861	6.815×10^{-5}
6	0.83	0.89	0.86	0.86	0.87	0.83	0.85	0.89	0.84	0.87	0.862	1.593×10^{-4}
7	1,04	1.06	1.03	1.01	1.05	1.08	1.07	1.06	1.03	1.06	1.046	2.816×10^{-4}
8	1.03	1.04	1.06	1.05	1.05	1.08	1.05	1.05	1.06	1.04	1.049	1.261×10^{-4}
9	1.01	1.04	1,07	1.04	1.03	1.06	1.01	1.08	1.06	1.05	1.052	1.2384×10^{-4}
10	0.56	0.54	0.6	0.57	0.55	0.51	0.6	0.6	0.53	0.57	0.560	5.763×10^{-4}
11	0.54	0.54	0.56	0.58	0.57	0.57	0.58	0.56	0.54	0.57	0.564	1.192×10^{-4}
12	0.60	0.58	0,58	0.60	0.62	0.55	0.59	0.56	0.57	0.56	0.570	1.952×10^{-4}
13	0.84	0.83	0.86	0.86	0.88	0.84	0.86	0.83	0.89	0.88	0.869	2.941×10^{-4}
14	0.86	0.84	0.85	0.86	0.87	0.85	0.88	0.87	0.88	0.87	0.869	6.253×10^{-5}
15	0,86	0.87	0.87	0.87	0.86	0.88	0.88	0.87	0.87	0.87	0.870	1.512×10^{-5}
16	1.05	1.04	1.05	1.08	1.02	1.09	1.00	1.07	1.02	1.06	1.049	5.542×10^{-4}
17	1,04	1.02	1.05	1.02	1.03	1.03	1.06	1.02	1.04	1.04	1.039	7.744×10^{-5}
18	1.01	1.06	1.02	1.06	1.01	1.03	1.01	1.02	1.03	1.06	1.036	2.297×10^{-4}
19	0.58	0.57	0.56	0.55	0.55	0.57	0.59	0.56	0.58	0.57	0.571	8.276×10^{-5}
20	0,58	0.59	0.58	0.59	0.55	0.57	0.58	0.56	0.56	0.57	0.567	7.219×10^{-5}
21	0.57	0.55	0.54	0.55	0.56	0.56	0.54	0.55	0.55	0.59	0.563	2.604×10^{-4}
22	0.84	0,84	0.84	0.84	0.84	0.86	0.85	0.84	0.85	0.85	0.849	1.765×10^{-5}
23	0.84	0.84	0.84	0.85	0.85	0.86	0.85	0.86	0.86	0.86	0.855	1.811×10^{-5}
24	0.86	0.86	0.84	0.82	0.89	0.86	0.81	0.85	0.84	0.85	0.846	1.557×10^{-5}
25	1.02	0.99	1.01	1.03	0.99	1.01	1.03	1.06	1.02	1.04	1.032	2.424×10^{-4}
26	1.06	1.04	1.02	1.04	1.06	1.02	1.06	1.01	1.02	1.04	1.033	1.733×10^{-4}
27	1.02	1.01	0.99	0.99	1.03	1.02	1.02	1.02	1.01	0.99	1.008	$1,287 \times 10^{-4}$

pitch $S_{o,i}$, the deforming force $F_{d,i}$ and the feed rate $f_{in,i}$. According to the results of a full-factor experiment (FFE) 3^3 in coded values, $b_{(x_1,x_2,x_3)} = f(S_{o,i}, F_{d,i}, f_{in,i})$:

$$b_{(x_1,x_2,x_3)} = 0.867 + 0.0015x_1 + 0.235x_2 - 0.0058x_3 - 0.00625x_1x_2 - 0.00975x_1x_3 - 0.008x_2x_3 + 0.004x_1^2 - 0.064x_2^2 - 0.0075x_3^2, \quad (3)$$

where x_1 is the coded value of the axial pitch; x_2 is the coded value of the deforming force; x_3 is the coded value of the feed rate.

All coefficients of the regression Equation (3) are significant. After transforming and simplifying Expression (3), a regression Equation (4) with natural coefficients is obtained:

$$b_{(S_{o,i}, F_{d,i}, f_{in,i})} = 0.0261 + 9.5 \cdot 10^{-3} S_{o,i} + 2.6287 \cdot 10^{-3} F_{d,i} + 1.389 \cdot 10^{-4} f_{in,i} - 3.125 \cdot 10^{-5} S_{o,i} F_{d,i} - 1.95 \cdot 10^{-5} S_{o,i} f_{in,i} - 8 \cdot 10^{-8} F_{d,i} f_{in,i} + 4 \cdot 10^{-3} S_{o,i}^2 - 1.6 \cdot 10^{-6} F_{d,i}^2 - 3 \cdot 10^{-8} f_{in,i}^2. \quad (4)$$

The derived regression equations (3) and (4) can be used to predict the groove width after the ball burnishing process. The axial pitch of roughness $S_{o,i}$, deforming force $F_{d,i}$ and feed rate $f_{in,i}$ vary within the following variation range of the input factors: $2 \leq S_{o,i} \leq 4$ (mm); $200 \leq F_{d,i} \leq 600$ (N); $500 \leq f_{in,i} \leq 1500$ (mm/min). The response surfaces obtained from the regression equation (4), which shows the relations between the groove width and the ball burnishing parameters, are shown in Figures 6–8.

As can be seen from the response surfaces graphs shown in Figures 6–8, the greatest contribution (99.7%) to the grooves width has the ball burnishing parameter deforming force F_d . The feed rate and the axial pitch have much smaller effect on the optimization parameter (together in range of up to 0.3%). This is confirmed by the response surfaces shown in Figures 6 and 8. Such behavior fully corresponds to the theoretical formulations and the results from other similar studies (Kyrychok & Lototska, 2011), in which those regime parameters have the strongest influence on the degree of deformation of the material surface layer.

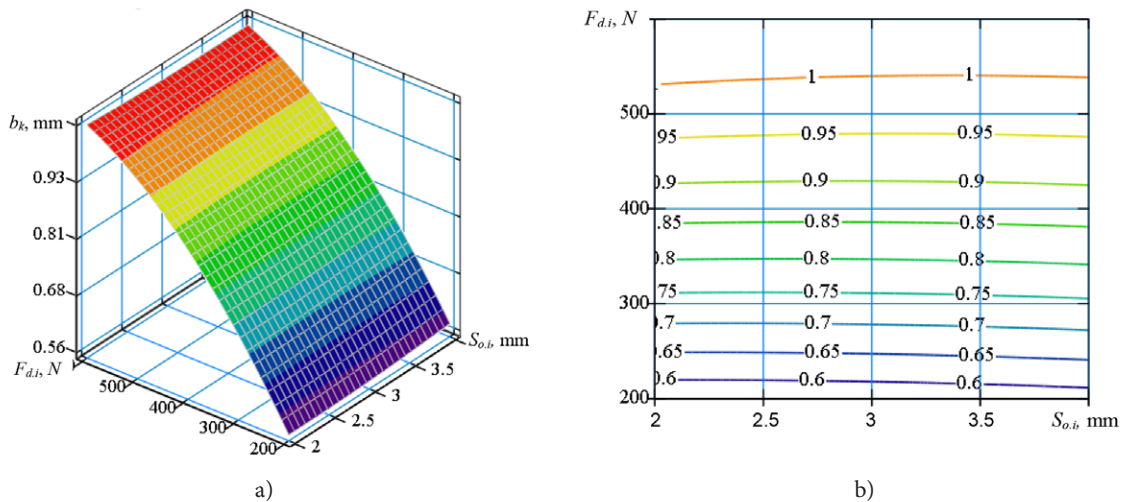


Figure 6. Response surface (a) and two-dimensional cross-section of the response surface (b) in the dependence of the groove width versus variation of the axial pitch $S_{o,i}$ and the deforming force $F_{d,i}$ ($f_{in,i} = 1000$ mm/min)

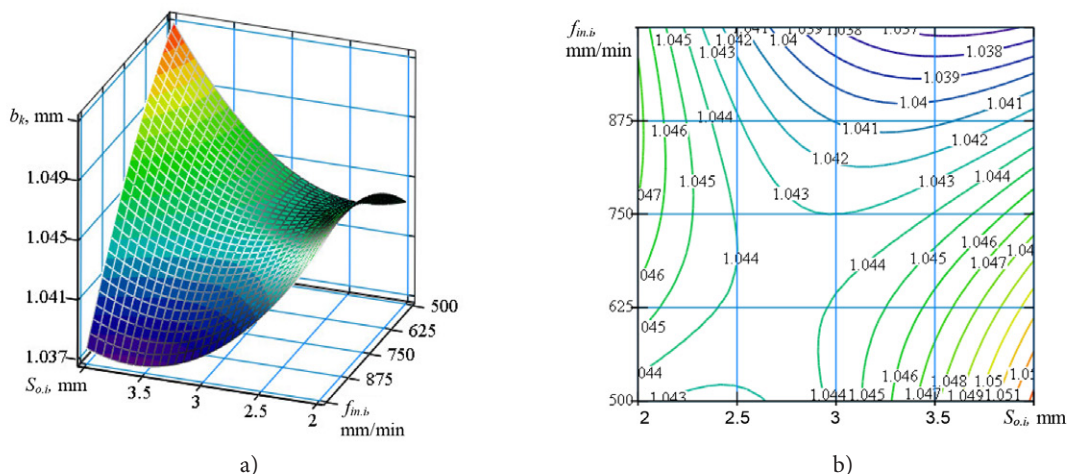


Figure 7. Response surface (a) and two-dimensional cross-section of the response surface (b) in the dependence of the groove width versus variation of the axial pitch $S_{o,i}$ and the feed rate $f_{in,i}$ ($F_{d,i} = 600$ N)

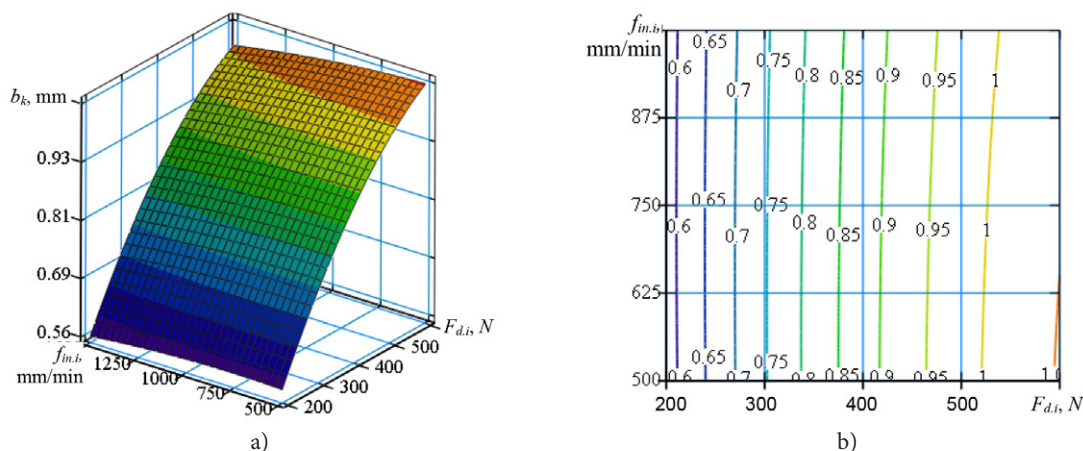


Figure 8. Response surface (a) and two-dimensional cross-section of the response surface (b) in the dependence of the groove width versus the variation of the deforming force $F_{d,i}$ and the feed rate $f_{in,i}$ ($S_{o,i} = 4$ mm)

By comparing the influence of the feed rate and the axial pitch (Figure 7), it can be seen that when the feed rate is at its low values $f_{in,i} = 500$ mm/min, the axial pitch $S_{o,i} < 3.5$ mm, and the deforming force $F_{d,i} = 600$ N are at their highest values, and the groove width reaches its maximum. This is because when the feed rate is at its minimum value (i.e. $f_{in,i} = 500$ mm/min), the time, during which the deforming force acts on the material surface layer, is the longest. Thus, the degree of plastic deformation will also be the highest.

The axial pitch distance $S_{o,i}$ has the smallest contribution to the width of the obtained grooves, because this factor influences the location of the deforming tool trajectory, rather than the deformation state of the material surface layer.

Conclusions

Partially regular microreliefs are formed by using different ball burnishing regime parameters on the face surfaces of test rotary body using a CNC-milling machine (HAAS TM-1). A contemporary vibration-free method based on the previously developed mathematical models is used to form partially regular microreliefs by ball burnishing operation. The specially designed deforming tool, which has the ability to adjust the deforming force of up to 3200 N and to measure its magnitude during the ball burnishing operation, is also used. This experimental research confirms the applicability of the mathematical models for calculating the coordinates of the toolpaths point.

Based on the results of the full-factorial experimental research, the influence of deforming force, feed rate and axial pitch on the plastically deformed grooves is derived. The average width of the PRMR groove formed on the test part face surface was considered. The regression dependences, the response surfaces and the corresponding contour plots are also obtained and discussed. They reveal the influence of these regime parameters on the groove width.

As result, it is found that the magnitude of deforming force has the greatest impact on the groove width and,

respectively, on the relative contact. Feed rate has a lower effect, and the least contribution comes from the axial pitch between adjacent toolpaths.

The present work should be considered mainly as a physical approbation of the mathematical models for generating toolpaths for partially RMRs. The new contemporary approach using CNC-equipment, which is developed by the co-authors team, is also considered. This approach is used to study the physical formation of partially RMRs on surfaces of real parts. The future work will be focused on determining the influence of microrelief formation conditions on the surface roughness and hardness in order to investigate the potential application of the partial RMR in various workpieces used in the construction of production equipment, vehicles, aircrafts, etc.

References

- Bakhtizin, R., Urazakov, R., Latypov, M., Ishmukhametov, B., & Narbutovskikh, A. (2017). The influence of regular microrelief forms on fluid leakage through plunger pair of sucker rod pump. *Oil Industry Journal*, 4, 113–116. (in Russian). <https://doi.org/10.24887/0028-2448-2017-4-113-116>
- Cao, C., Zhu, J., & Tanaka, T. (2020). Influence of burnishing process on microstructure and corrosion properties of Mg alloy AZ31. In S. Itoh & S. Shukla (Eds.), *Advanced surface enhancement. Proceedings of the 1st International Conference on Advances Surface Enhancement (INCASE 2019). Lecture Notes in Mechanical Engineering* (pp. 97–107). Springer. <https://doi.org/10.1007/978-981-15-0054-1>
- Diltemiz, S., Uzunonut, Y., Kushan, M., & Celik, O. (2009). Effect of dent geometry on fatigue life of aircraft structural cylinder part. *Engineering Failure Analysis*, 16(4), 1203–1207. <https://doi.org/10.1016/j.engfailanal.2008.07.017>
- Dyshunskiy, V. (1998). *Basics of the scientific research. Theory and workshop with softwar*. KPI.
- Dzyura, V. O., Maruschak, P. O., Zakiev, I. M., & Sorochak, A. P. (2017). Analysis of inner surface roughness parameters of load-carrying and support elements of mechanical systems. *International Journal of Engineering, Transactions B: Applications*, 30(8), 1170–1175.

- Dzyura, V. (2020). Modeling of partially regular microreliefs formed on the end faces of rotation bodies by a vibration method. *Ukrainian Journal of Mechanical Engineering and Materials Science*, 6(1), 30–38. <https://doi.org/10.23939/ujm2020.01.030>
- Hamdi, A., Merghache, S. M., Aliouane, T. (2020). Effect of cutting variables on bearing area curve parameters (BAC-P) during hard turning process. *Archive of Mechanical Engineering*, 67(1), 73–95.
- Kindrachuk, M., Radionenko, O., Kryzhanovskiy, A., & Marchuk, V. (2014). The friction mechanism between surfaces with regular micro grooves under boundary lubrication. *Aviation*, 18(2), 64–71. <https://doi.org/10.3846/16487788.2014.926642>
- Kolker, Y. (1976). *Mathematical analysis of machine parts working accuracy*. Technika.
- Korneev, V. M. (2009). *Konstrukciya i osnovy ekspluatatsii letatelnyh apparatov: konspekt lekciy*. UVAU GA(i). (in Russian).
- Krishnaiah, K., & Shahabudeen, P. (2012). *Applied design of experiments and Taguchi methods*. PHI Learning Private Limited.
- Kryvyi, P., Dzyura, V., Tymoshenko, N., & Krypa, V. (2014, 9–13 June). Technological heredity and accuracy of the cross-section shapes of the hydro-cylinder cylindrical surfaces. In *International Conference on Materials and Processing and the 42nd North American Manufacturing Research Conference*. Paper No. MSEC2014-3946. Detroit. <https://doi.org/10.1115/MSEC2014-3946>
- Kyrychok, P., & Lototska, O. (2011). Experimental studies of the geometric parameters of cylindrical parts of printing machines in the time of complex processing. *Journal of Tekhnolohiia i Tekhnika Drukarkstva*, 3(33), 4–12. (in Ukrainian). [https://doi.org/10.20535/2077-7264.3\(33\).2011.52142](https://doi.org/10.20535/2077-7264.3(33).2011.52142)
- Kuzmin, Yu., Pompeev, K., & Tselishchev, A. (2015). Application of milling machine to impression a regular microrelief on preform surface. *Journal of Instrument Engineering*, 58(4), 273–277. <https://doi.org/10.17586/0021-3454-2015-58-4-273-277>
- Lazarev, S. V., Khusnutdinov, R. F., Tolmachev, A. A., & Velikanov, A. V. (2008). *Aircraft Towing Device*, 1–5. <https://www.freepatent.ru/patents/2361786>
- Leshkenova, L. (2002). *Increasing the productivity of the processing process and improving the operational properties of the surfaces of holes by the method of surface plastic deformation with the formation of a regular microrelief* [Dissertation of Candidate of Sciences, Saratov State Technical University]. Saratov.
- Nagit, G., Dodun, O., Slatineanu, L., Ripanu, M., Mihalache, A., & Hrituc, A. (2020). Influence of some process input factors on the main dimensions of the grooves generated during the ball vibroburnishing. In *IOP Conference Series: Materials Science and Engineering*, 968, 012007. <https://doi.org/10.1088/1757-899X/968/1/012007>
- Nalbant, M., Gökaya, H., & Sur, G. (2007). Application of Taguchi method in the optimization of cutting parameters for surface roughness in turning. *Materials & Design*, 28(4), 1379–1385. <https://doi.org/10.1016/j.matdes.2006.01.008>
- Ouyang, X., Gao, F., Yang, H., & Wang H. (2011). Two-dimensional stress analysis of the aircraft hydraulic system pipeline. In *Proceedings of the Institution of Mechanical Engineers Part G: Journal of Aerospace Engineering*, 226(5), 532–539. <https://doi.org/10.1177/0954410011413011>
- Pogodayev, V. (2004). *Technological support of surface parameters with partially regular microrelief of friction pair parts* [Dissertation of Candidate of Sciences, Omsk State Technical University]. Omsk. (in Russian).
- Radionenko, O., Kindrachuk, M., Tisov, O., & Kryzhanovskiy, A. (2018). Features of transition modes of friction surfaces with partially regular microrelief. *Aviation*, 22(3), 86–92. <https://doi.org/10.3846/aviation.2018.6204>
- Schneider, Yu. (1984). Formation of surfaces with uniform micropatterns on precision machine and instruments parts. *Precision Engineering*, 6(4), 219–225. [https://doi.org/10.1016/0141-6359\(84\)90007-2](https://doi.org/10.1016/0141-6359(84)90007-2)
- Slavov, S. D., Dimitrov, D. M., & Konsulova-Bakalova, M. Iv. (2021). Advances in burnishing technology. In *Advanced Machining and Finishing* (pp. 481–525). Elsevier. <https://doi.org/10.1016/B978-0-12-817452-4.00002-6>
- Slavov, S., & Dimitrov, D. (2018). A study for determining the most significant parameters of the ball-burnishing process over some roughness parameters of planar surfaces carried out on CNC milling machine. In *MATEC Web of Conferences*, 178, 02005. <https://doi.org/10.1051/mateconf/201817802005>
- Slavov, S., Dimitrov, D., & Iliev, I. (2020). Variability of regular relief cells formed on complex functional surfaces by simultaneous five-axis ball burnishing. *UPB Scientific Bulletin, Series D: Mechanical Engineering*, 82(3), 195–206.
- Slavov, S., & Iliev, I. (2016). Design and fem static analysis of an instrument for surface plastic deformation of non-planar functional surfaces of machine parts. *Fiability & Durability, Editura "Academica Brâncuși"*, 2, 3–9.
- Stadnychenko, V., & Varvarov, V. (2019). Results of theoretical and experimental researches of anomalous low friction and wear in tribosystems. *Advances in Material*, 8(4), 156–165. <https://doi.org/10.11648/j.am.20190804.14>
- State Standard of the Union of USSR. (1988). *Surfaces with regular microshape. Classification, parameters and characteristics (GOST 24773-81)*. Moscow. (in Russian).
- Voronkov, R. V. (2019). *Metody i sredstva povysheniya effektivnosti provedeniya resursnyh ispytaniy naturnykh aviacionnykh konstrukci* [Avtoreferat dissertatsii na soiskanie uchenoj stepeni kandidata tehnikeskikh nauk po spec. 05.07.03 – Prochnost i teplovye rezhimy letatelnyh apparatov]. Centralnyin Aerodinamicheskij Institut imeni professora N.E. Zhukovskogo, Zhukovskij. (in Russian).
- Wang, S., Tomovic, M., & Liu, H. (2016). Chapter 2 – Aircraft hydraulic systems. In *Commercial aircraft hydraulic systems* (pp. 53–60). Academic Press. <https://doi.org/10.1016/B978-0-12-419972-9.00002-4>
- Wu, W., Chen, G., Fan, B., & Liu, J. (2016). Effect of groove surface texture on tribological characteristics and energy consumption under high temperature friction. *PLoS ONE*, 11(4), e0152100. <https://doi.org/10.1371/journal.pone.0152100>
- Zhang, Y., Zeng, L., Wu, Z., Ding, X., & Chen, K. (2019). Synergy of surface textures on a hydraulic cylinder piston. *Micro Nano Letters*, 14, 424–429. <https://doi.org/10.1049/mnl.2018.5535>
- Zerti, O., Yallese, M., Khettabi, R., Chaoui, K., & Mabrouki, T. (2017). Design optimization for minimum technological parameters when dry turning of AISI D3 steel using Taguchi method. *The International Journal of Advanced Manufacturing Technology*, 89(5–8), 1915–1934. <https://doi.org/10.1007/s00170-016-9162-7>